Design and fabrication of organic solar cells structured via nanoimprint lithography

O Wiedenmann, A Abdellah, G Scarpa and P Lugli

Institute for Nanoelectronics, Technische Universität München, D-80333 Munich, Germany

E-mail: lugli@tum.de

Abstract. A theoretical analysis based on a drift-diffusion simulation method is performed for investigating device performances of nanostructured organic solar cells. The results show an increase of the short-circuit current density, which can be attributed to the increased interface area. Patterning via nanoimprint techniques is demonstrated, which constitutes the first step towards the realization of bulk-heterojunction organic solar cells with controlled morphology.

1. Introduction

In recent years, research and development in the field of organic semiconducting materials has advanced tremendously, driven by the potential for a variety of low cost, large area devices with attractive market perspectives. Ever since the discovery of conductivity and semi-conductivity in polymers [1] as well as the discovery of metallic conductivity in poly-acetylene in 1977 [2], the electrical properties of various small molecules and polymers have been investigated. This paved the way for the realization of organic light-emitting diodes (OLED), photodiodes, transistors and sensors. The field of organic optoelectronics has become one of the most promising for research and for industry. It is therefore not surprising that it is in this field where the first commercial products like OLED displays have emerged. Utilizing the full range of advantages offered by organic semiconductor technology (e.g. large-area, cheap manufacturing, flexible substrates), solar cells based on organic materials can potentially be manufactured in mass production at lower costs with respect, e.g., to silicon [3] since they do not require high deposition temperatures, complex processing or clean room environments. However, up to now the efficiencies of organic solar cells cannot compete with conventional photovoltaics. One major challenge is the control of the interfacial area between donor-acceptor materials. In fully organic solar cells two organic components with different electron and hole affinities are mixed [3]. Generally the fabrication methods (such as solution processing and vacuum sublimation) used for preparing the active films of these components do not allow high control over the phase separation of the organic layers. A promising alternative is provided by nanopatterning techniques and in particular by nanoimprint lithography [4-7]. This method allows one to structure organic layers in the nanometer scale and enables the tuning of the interfacial area between the two organic materials. In this paper, we discuss the influence of morphology on the performance of organic solar cells via a two dimensional simulation. In addition, we show how nanoimprinting can realize patterning of the active layers down to the required nanometer scale.

2. Methods

2.1. Nanoimprint lithography

Nanoimprint lithography (NIL) can be used for structuring thin P3HT layers. This technique would allow the realization of ordered heterostructure solar cells [6,7] using P3HT as donor material, for further improving the efficiency of these devices. In order to fabricate heterostructures based on the P3HT/PCBM material system, one should be able to deposit PCBM on top of P3HT layers. However, the use of spin-coating techniques could be difficult, since successively deposited layers would eventually destroy the layer underneath. Our experiments revealed that by using different solvents for the two polymers, a bilayer structure of P3HT and PCBM can be realized. Our films were spin coated at 1500 rpm for 20 s from a chloroform solution (with a concentration of 0.5 % by weight) onto 0.5 μm-thick polished glass covered by a PEDOT:PSS (Baytron P purchased by H. C. Starck) layer, which was spun on the substrates prior to deposition of the P3HT layer (2000 rpm for 20 s baked at 150°C for 15 min). All films were deposited under nitrogen atmosphere and no other thermal treatment was applied after depositing the P3HT.
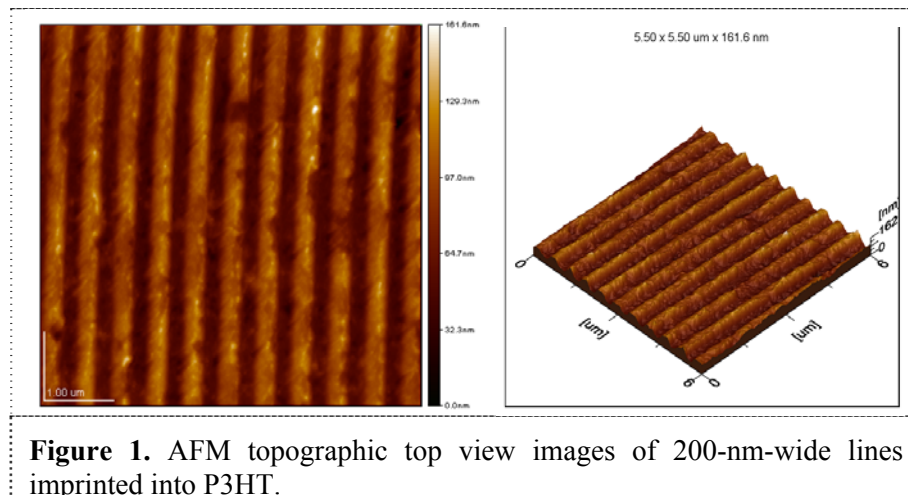

Figure 1. AFM topographic top view images of 200-nm-wide lines imprinted into P3HT.

After deposition, the samples were placed on the chamber of a commercial (Obducat 2.5 inch) NIL tool with the mold manually placed upside down onto the imprint polymer layer. Imprint duration, temperature and pressure were computer-controlled, in-situ monitored, and can be preset. Figure 1 shows topographic AFM images of imprinted P3HT polymer surfaces structured with the NIL process described above, with grating patterns comprising 200-nm-wide lines. The imprint temperature was 180°C. The surface structure of the P3HT film layer shows good feature transfer quality with an imprint depth of approximately 80 nm and rounded sidewalls.

2.2. Simulation method

Our simulation is based on the drift diffusion approach implemented in the commercial software tool SENTAURUS[TM], which is a widely used and well-known software package developed for inorganic semiconductors [8]. It is a multidimensional, electro-thermal, mixed-mode device and circuit simulator designed to simulate inorganic one-dimensional, two-dimensional and three-dimensional semiconductor devices. The self-consistent numeric scheme solves the Poisson equation coupled to the drift-diffusion and continuity equations while considering van-Neumann type boundary conditions for contacts and geometry. This approach showed already good agreement for organic bulk heterojunction solar cells [9]. In order to account for the special nature of organic semiconductors, input parameters such as the energy of the transport levels and the mobility needed to be adjusted [10]. Furthermore, we

have implemented a number of physical models (e.g. field-dependent and density-dependent mobility, Langevin-type recombination), which are essential in organic materials. The material parameters used for the donor material (P3HT), the acceptor material (PBCM) and the blend structure (P3HT:PCBM) are shown in Table 1. To introduce the blend into our simulations, we have combined the properties of both P3HT and PCBM in a virtual semiconductor. The LUMO and HOMO levels are taken from PCBM and P3HT, respectively, as illustrated in the inset of Figure 2. Figure 2 demonstrates the precision that we can obtain in the reproduction of experimental current-voltage characteristics of BHJ photodiodes. In the implementation of the simulations, it has been a key success factor to derive a suitable material model that would describe the polymer bulk heterojunction in the blend material. The analyzed device has a 200 nm active layer of P3HT:PCBM blend contacted by ITO and Calcium electrodes. In the case of nanostructured solar cells, in order to take into account the effects of exciton-dissociation at the interface between donor and acceptor material, a 10 nm region along the interface has been defined as virtual semiconductor (as explained above). The absorbing region defined as a virtual semiconductor is indicated by the dotted area along the donor/acceptor interface in the inset of Figure 3. This allowed us to mimic exciton processes (generation, diffusion and dissociation) and to properly account for the separation of the charges generated from exciton-dissociation and their further contribution to the carrier density at the respective energy levels of the materials (inset of Figure 2). In other words, incident photons generate excitons, which start to diffuse in the material. As assumption, only those excitons generated within the exciton diffusion length from the interface can dissociate. After dissociation, a free electron can move in the LUMO of the acceptor (PCBM), while a free hole can travel in the HOMO of the donor (P3HT). Finally, the carriers are collected by the respective metal contacts.

Table 1. Virtual semiconductor parameters used for the P3HT:PCBM blend.

	P3HT	virtual semiconductor (blend structure)	PCBM
LUMO [eV]	3.0	3.7	3.7
HOMO [eV]	5.0	4.86	6.1
Band gap [eV]	2.0	1.16	2.4
Hole mobility [cm^2/Vs]	1.0e-3	1.0e-3	1.0e-5
Electron mobility [cm^2/Vs]	1.0e-5	1.0e-3	1.0e-3
Effective absorption [cm^{-1}]	2.0e4	2.0e4	2.0e4
Density of states [cm^{-3}]	5.0e20	5.0e20	5.0e20
Carrier lifetime [s]	5.0e-7	5.0e-7	5.0e-7

3. Results

The current-voltage characteristics of organic solar cells with different interface geometries are shown in Figure 3, while the insets show the schematic cross-section of the devices. A bilayer structrure of 100 nm P3HT and 100 nm PCBM is simulated as reference cell (Table 2). The nanostructured devices have a total active layer thickness of 200 nm, which is divided into a structured region of 100 nm height (parameter h in the inset of Figure 3) embedded in a 50 nm thick donor and acceptor layer, respectively. The simulated widths (parameter w in the inset of Figure 3) are indicated in Table 2.

Whereas the open circuit voltage V_{OC} of the devices remains constant in agreement with previous findings [5], the short circuit current density J_{SC} is rising with larger interface areas. This fact can be explained with the increasing number of excitons reaching the donor/acceptor interface in order to dissociate, thus generating more carriers.

Table 2 shows a comparison between the sizes of the interface area of the active region (where exciton splitting is assumed) and the respective short circuit current density values of the devices extracted from our simulations. It is worth to observe that the correlation between interface area and short circuit current density is quite accurate.
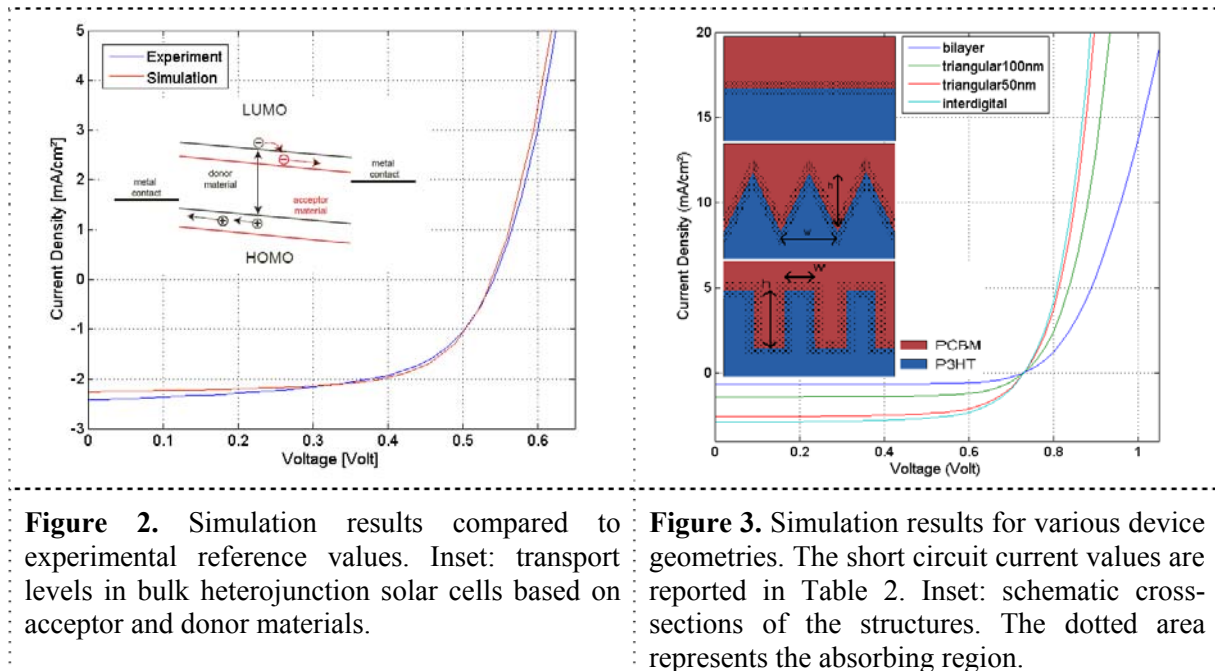

Figure 2. Simulation results compared to experimental reference values. Inset: transport levels in bulk heterojunction solar cells based on acceptor and donor materials.

Figure 3. Simulation results for various device geometries. The short circuit current values are reported in Table 2. Inset: schematic cross-sections of the structures. The dotted area represents the absorbing region.

Table 2. Comparison of the different geometries with the calculated interface areas.

	A/A_0	J_{SC}	J_{SC}/J_{SC0}	V_{OC}
Bilayer (reference cell)	1	0.65	1	0.73
Triangular (w=50 nm)	2.2	1.41	2.17	0.73
Triangular (w=25 nm)	4.0	2.58	3.97	0.73
Interdigital (w=25 nm)	4.15	2.90	4.46	0.73

4. Conclusions

The simulation will help understand the physical models and the principal effects of device specific parameters, as simulation variables for the materials and their impact on the results can be illustrated. The ability to accurately simulate the electrical and optical properties of solar cells based on organic semiconducting materials will aid in the design process.

References
[1]   Shirakawa H, Louis EJ, Macdiarmid AG, Chwan K, Heeger AJ, Chem. Comm. **16**, 578 (1977).
[2]   Chiang CK, et al., Phys. Rev. Lett. **39**, 1098 (1977).
[3]   Thompson BC, Frechet JMJ, Angew. Chem. Int. Ed. **47**, 58 (2008).
[4]   Chou SY, Appl. Phys. Lett. **67**, 3114 (1995).
[5]   Kim M, et al., Appl. Phys. Lett. **90**, 123113 (2007).
[6]   Na S, et al., Appl. Phys. Lett. **91**, 173509 (2007).
[7]   Cheyns D, et al., Nanotechnology **19**, 424016 (2008).
[8]   www.synopsys.com
[9]   Waldauf C, Schilinsky P, Hauch J, Brabec CJ, Thin Solid Films **451–452**, 503 (2004).
[10] Bolognesi A, Di Carlo A, J. of Comp. Electr. **2(2-4)**, 297 (2003).